European Journal of Pharmaceutics and Biopharmaceutics 80 (2012) 508–517

Contents lists available at SciVerse ScienceDirect

European Journal of Pharmaceutics and Biopharmaceutics

journal homepage: www.elsevier.com/locate/ejpb

Research paper

Self-assembled biotransesterified cyclodextrins as Artemisinin nanocarriers – I: Formulation, lyoavailability and *in vitro* antimalarial activity assessment

Josias B.G. Yaméogo [a,c], Annabelle Gèze [a,*], Luc Choisnard [a], Jean-Luc Putaux [b], Adama Gansané [d], Sodiomon B. Sirima [d], Rasmané Semdé [c], Denis Wouessidjewe [a]

[a] DPM, UMR CNRS 5063, ICMG FR 2607, Faculty of Pharmacy, University of Grenoble, France
[b] CERMAV, UPR CNRS 5301, ICMG FR 2607, Grenoble, France
[c] UFR/SDS, University of Ouagadougou, Burkina Faso
[d] Centre National de Recherche et de Formation sur le Paludisme (CNRFP), Burkina Faso

ARTICLE INFO

Article history:
Received 8 November 2011
Accepted in revised form 19 December 2011
Available online 30 December 2011

Keywords:
Amphiphilic cyclodextrins
Nanocarriers
Artemisinin
Malaria
Plasmodium falciparum
Cryo-TEM

ABSTRACT

We recently reported a one-step transesterification of cyclodextrins (CDs) by vinyl-acyl fatty esters catalyzed by thermolysin. By using the solvent displacement method and depending on the experimental conditions, the CD derivatives grafted with decanoic alkyl chains (CD-C_{10}) yielded either nanosphere or nanoreservoir-type systems with a size ranging from 70 to 220 nm. Both types of nanostructures were able to associate artemisinin (ART), a well-known antimalarial lipophilic drug. The formulation parameters were optimized to reach stable and high ART dosage corresponding to drug levels of 0.3 and 1.6 mg mL^{-1} in the colloidal suspension, for the spherical and reservoir-type nanosystems, respectively. PEG surface-decorated nanoparticles were also prepared by co-nanoprecipitation of PEG fatty acid esters and CD-C_{10} molecules. The integration of the PEGylated amphiphiles within the CD-C_{10} nanostructures did not influence the ART lyoavailability. Both types of ART-loaded nanosystems showed a sustained *in vitro* release profile over 96 (nanoreservoirs) and 240 h (nanospheres). Finally, the *in vitro* antimalarial activity was evaluated using the lactate dehydrogenase assay. ART-containing colloidal suspensions inhibited the growth of cultured *Plasmodium falciparum*, both multi-resistant K1 and susceptible 3D7 strains with IC_{50} values (2.8 and 7.0 ng mL^{-1}) close to those of reference ART solution. These colloidal nanosystems based on CD derivatives and containing ART may provide a promising alternative formulation for injectable use of ART.

1. Introduction

Malaria is a major public health problem in several tropical countries causing about 500 million clinical cases and 3 million deaths each year, essentially children and pregnant women. The severe and complicated stages have a mortality rate between 20% and 50%. The *Plasmodium falciparum* parasite is responsible for the most serious form of the disease, resulting in rapid deterioration of the patient condition together with the development of a number of life-threatening complications [1]. To face the resistance of *P. falciparum* against usual drugs like chloroquine, the challenge lies in finding alternative therapies, especially for high-risk groups.

Artemisinin (ART), an endoperoxide sesquiterpene lactone antimalarial drug (Fig. 1) isolated from a Chinese medicinal herb (*Artemisia annua*), has a fast action against chloroquine-sensitive and chloroquine-resistant strains of *P. falciparum*, making it very effective in the treatment of multidrug-resistant malaria. However, its poor aqueous solubility, short half-life, and high first-pass metabolism limit its use in therapeutics [2,3]. Many studies were carried out with the aim of enhancing ART solubility and/or bioavailability. Among these investigations, Wong et al. demonstrated that ART solubility, dissolution and oral bioavailability could be increased through inclusion complexes with β- and γ-cyclodextrins (CDs) [4,5]. The spray-drying of ART with maltodextrins has also been successfully tested to enhance the aqueous solubility of ART [6]. The use of lipid nanocarriers such as liposomes and nanocapsules to improve delivery of antimalarial compounds such as the lipophilic ART derivative artemether, chloroquine, and halofantrine has also been established [7–10].

Recently, we successfully synthesized α-, β-, and γ-CD fatty esters grafted on the secondary face with C_4 to C_{14} aliphatic chains, by a one-step transesterification using thermolysin as biocatalyzer and vinyl-acyl esters as alkyl chains donor [11,12]. These CD derivatives have been shown to self-assemble and form stable supramolecular matrix-type or reservoir-type particles in the conditions of

* Corresponding author. DPM, UMR CNRS 5063, ICMG FR 2607, Faculty of Pharmacy, University of Grenoble, France. Tel.: +33 476635301; fax: +33 476635322.
E-mail address: annabelle.geze@ujf-grenoble.fr (A. Gèze).

0939-6411/$ - see front matter © 2012 Elsevier B.V. All rights reserved.
doi:10.1016/j.ejpb.2011.12.007

nanoprecipitation [11–13]. Some of these derivatives formed original multilayered nanostructures, foreshadowing different drug localizations in the nanostructure [11].

The purpose of the present study was to investigate the potential of the latest self-assembled bio-transesterified CD-based nanocarriers as ART delivery systems for an intravenous route. The rationale behind the use of these nanodevices is related to their size and their ability to associate lipophilic drugs [13,14]. The objective of our study was twofold: (i) to improve the ART dosage through its association with CD esters-based nanocarriers, (ii) to ensure a sufficient blood circulation time of the nanocarriers through their surface decoration, which is a prerequisite to reach infected erythrocytes after systemic administration. This paper reports on the formulation, the physicochemical and morphological characterization and *in vitro* evaluation (release kinetics and antimalarial activity) of ART-loaded nanoaggregates.

First, we synthesized and characterized fatty acid esters of β- and γ-CD by a biocatalysis method, using the vinyl decanoate as donor of alkyl chain. The ability of these derivatives to self-organize into submicronic structures was assessed using the solvent displacement method. In the second part, the effect of some formulation parameters on the ART entrapment by β- or γ-CD-C_{10} based nanospheres was evaluated. The ART incorporation was subsequently extended to the nanoreservoir structures of γ-CD-C_{10} in order to evaluate the interest of both nanovehicles. Third, the integration of PEG esters in the formulation was investigated in order to prepare PEG surface-decorated particles with a prolonged blood circulation time. The last part of this study was devoted to *in vitro* testing of formulations selected on the basis of established criteria, namely the drug incorporation rate and the physicochemical stability.

2. Materials and methods

2.1. Materials

Thermolysin (EC 3.4.24.27), a protease type × isolated from *Bacillus thermoproteolyticus rokko*, anhydrous DMSO (99%), vinyl decanoate (95%), Artemisinin ($C_{15}H_{22}O_5$, 98%, Mw = 282.3 g mol^{-1}), RPMI 1640 medium, Albumax® II (Lipid rich bovine serum albumin for cell culture), Gentamicin (for *in vitro* culture), HEPES buffer (pH 7.4), Giemsa solution, Chloroquine diphosphate (98%, Mw = 516 g mol^{-1}), and celite were obtained from Sigma–Aldrich (l'Isle d'Abeau Chesnes, France). Dihydro-Artemisinin and Quinine hydrochloride were purchased from Fluka (Sigma–Aldrich). β- and γ-CD (Kleptose®) were provided by Roquette (Lestrem, France). Montane® 80 (sorbitan mono-oleate) and Montanox® 80 (polysorbate 80, ethoxylated sorbitan mono-oleate) of pharmaceutical grade were kindly provided by Seppic (Castres, France). Miglyol® 812 N (caprilyc/capric medium chain triglycerides) and poloxamer 188 were obtained from Sasol (Witten, Germany). Benzyl benzoate was supplied by Cooper (Melun, France). Polyethylene glycol (PEG300, PEG400, PEG1500 and PEG4000) esters (dilaurate and stearate) were purchased from Stearinerie DuBois (France). The organic solvents were from VWR International (Lyon, France). *P. falciparum* strains K1 and 3D7 were supplied by London School of Hygiene and Tropical Medicine (London, England). Malstat reagent was made with 0.125% Triton X-100, 130 mM L-lactate, 30 mM Tris buffer, and 0.62 μM 3-acetylpyridine adenine dinucleotide. NBT/PES solution was made with 1.90 μM nitro blue tetrazolium and 0.24 μM phenazine ethosulfate. Water was freshly deionized in our laboratory.

2.2. Synthesis and characterization of β- and γ-CD-C_{10}

The β- and γ-CD fatty esters were biosynthesized according to the procedure previously reported involving thermolysin as biocatalyzer [11,12]. The β- and γ-CD fatty esters were obtained as a white powder and were analyzed by matrix-assisted laser desorption/ionization mass spectroscopy (MALDI-MS).

MALDI-MS data of β-CD-C_{10}: (m+Na^+)/z = 2083.0 (Relative Intensity: 22.0%) [decanoate β-CD ester with 6 chains], 2237.0 (Relative Intensity: 100%) [decanoate β-CD ester with 7 chains]. 2391.0 (relative intensity: 22.0%) [decanoate β-CD ester with 8 chains]. MALDI-MS data of γ-CD-C_{10}: (m+Na^+)/z = 2398.0 (relative intensity: 7.2%) [decanoate γ-CD ester with 7 chains], 2552.1 (relative intensity: 100%) [decanoate γ-CD ester with 8 chains], 2706.3 (relative intensity: 87.2%) [decanoate γ-CD ester with 9 chains], 2860.4 (Relative Intensity: 34.4%) [decanoate γ-CD ester with 10 chains], 3014.0 (relative intensity: 7.2%) [decanoate γ-CD ester with 11 chains]. From these results and according to a validated analytical method [15], the products are characterized by an average molar weight and a total degree of substitution (TDS) of 2714 g mol^{-1} for γ-CD-C_{10} (TDS 9.2) and 2314 g mol^{-1} for β-CD-C_{10} (TDS 7.6).

2.3. Preparation of colloidal suspensions

2.3.1. Nanospheres

Unloaded nanoparticles were prepared in triplicate using the solvent displacement method [11–13]. The influence of oligosaccharide ring size (β- or γ-) and hydrophilic surfactant (Montanox® 80 or poloxamer 188) on the particle physical characteristics was evaluated. ART-loaded nanoparticles were prepared in a similar way by introducing the drug in the acetonic phase. Two types of formulations were first prepared with an initial CD fatty ester concentration in the organic phase of 1 mg mL^{-1} (FI) or 2 mg mL^{-1} (FII). In a second study, a modified displacement method was investigated with γ-CD-C_{10} only (Fig. 2). The biosynthesized CD was either co-nanoprecipitated with ART (process 1) or introduced in an aqueous phase containing ART (process 3). In the cases of processes 2 and 4 (multi-step procedure), a second addition of γ-CD-C_{10} was performed on preformed ART-loaded nanospheres.

2.3.2. Nanoreservoir systems

Reservoir-type nanosystems were prepared by injecting an organic phase containing acetone (10 mL), γ-CD-C_{10}, benzyl benzoate, and a lipophilic surfactant, Montane® 80, into an aqueous phase containing distilled water (20 mL) added with a hydrophilic surfactant, Montanox® 80, under magnetic stirring (500 rpm) at 25 °C. The organic solvent was removed under reduced pressure and the suspension was concentrated until a final aqueous volume corresponding to 50–60% of initial distilled water volume. ART-loaded systems were prepared using an initial drug amount of 20 mg in the organic solution. All preparations (sphere and reservoir colloidal suspensions) were finally rendered isotonic with glucose solution.

2.3.3. PEGylated nanosystems

PEGylated ART-loaded nanosystems (nanospheres and nanoreservoirs) were formulated according to the previous conditions by

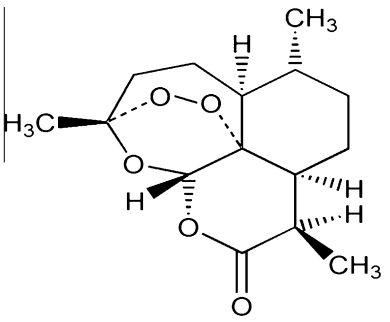

Fig. 1. The chemical structure of Artemisinin (ART).

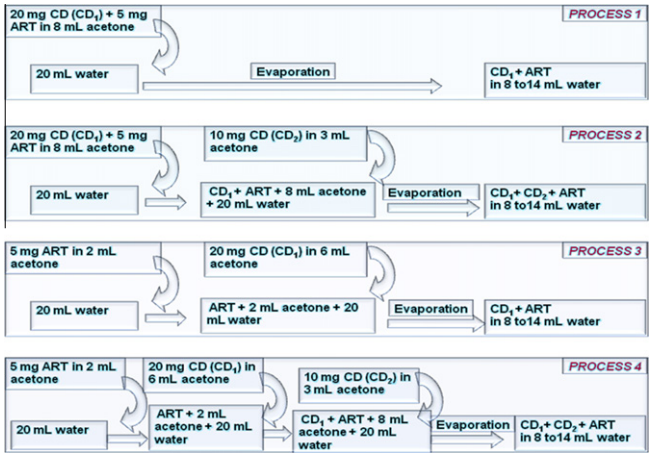

Fig. 2. CD and ART incorporation processes: one-step addition of CD (processes 1 and 3) or multi-step addition of CD (processes 2 and 4). Process 1 = addition of the acetonic phase (8 mL) containing CD (20 mg) and ART (5 mg) into the aqueous phase (20 mL deionized water) under stirring; Process 2 = first addition of an acetonic phase (8 mL) containing CD (20 mg) and ART (5 mg) in the aqueous phase (20 mL) and then addition of a second acetonic CD phase (10 mg in 3 mL); Process 3 = first addition of ART acetonic solution (5 mg in 2 mL) in the aqueous phase (20 mL) and then introduction of CD organic phase (20 mg in 6 mL of acetone); Process 4 = first addition of ART acetonic solution (5 mg in 2 mL) in the aqueous phase (20 mL) and then introduction of CD acetonic phase in two steps, 20 mg in 6 mL, then 10 mg in 3 mL. (For interpretation of the references to color in this figure legend, the reader is referred to the web version of this article.)

partially or totally substituting the hydrophilic surfactant by polyethylene glycol (PEG) esters. Free PEG ester in the supernatant was removed by gel chromatography. The PEGylated colloidal suspensions were passed through a Sephadex® G-75 columns (dry bead diameter = 40–120 μm, Sigma Aldrich, Sweden).

2.4. Physicochemical characterization of nanosystems

Mean size, polydispersity index (PI), and zeta potential measurements were performed after appropriate dilution by using a Zetasizer 3000 (10 mW HeNe laser at 632.8 nm) [11–13]. The morphology of the nanosystems was observed by transmission electron microscopy (TEM) after negative staining of the preparations with uranyl acetate, using a Philips CM200 'Cryo' microscope operating at 80 kV. The images were recorded on Kodak SO163 films. In addition, the reservoir systems were observed by cryo-TEM on thin vitrified films of the suspensions, according to the procedure described elsewhere [11].

2.5. Determination of drug loading

The amount of drug associated with the nanosystems was assessed as follows: the total concentration of ART recovered in the colloidal suspensions (Ct) was determined using HPLC-UV pre-column derivatization method [16]. The suspension was ultracentrifuged at 250,000 g (OPTIMA™ L-80 XP Beckman Coulter, rotor SW60 Ti) at 20 °C for 2 h (nanoreservoirs) or 1 h (nanospheres) to separate the particles from the supernatant. The ART concentration in supernatant (Cs) was determined by HPLC-UV in the same conditions. The drug recovery DR (%), the drug association DA (%), and the entrapment efficiency EE (%) were estimated as follows:

$$\mathrm{DR}\ (\%) = (\mathrm{Ct}/\mathrm{Ci}) \times 100 \quad (1)$$

where Ci is the theoretical drug concentration (initially introduced in the formulation).

$$\mathrm{DA}\ (\%) = (\mathrm{Ct} - \mathrm{Cs})/\mathrm{Ct} \times 100 \quad (2)$$

$$\mathrm{EE}\ (\%) = [\text{associated ART (mg)}/\text{Initial CD amount (mg)}] \times 100 \quad (3)$$

An HPLC-UV quantification at 260 nm was carried out at 35 °C with a 1 mL min^{-1} flow rate according to a validated method (r^2 = 0.9997, $y = 35880x - 20{,}550$) firstly described by Zhao [16]. After a derivatization step by alkaline hydrolysis at 50 °C (Fig. 3) and then neutralization in an acidic medium, the sample was analyzed using a HPLC system constituted by a Varian Prostar pump, a Varian 9050 UV detector, and a Varian Prostar auto-injector model 400. A column Nucleosil 100 C_{18} (250 × 4.6 mm; 5 μm particle size) from VWR International and a mixture of phosphate buffer (K_2HPO_4 + KH_2PO_4, 0.05 M, pH 6.3) and methanol (55:45, v/v) were used as stationary and mobile phases, respectively.

2.6. Stability study

The suspensions were stored at room temperature during 30 days and their stability was evaluated in terms of appearance, particle size, polydispersity index, and drug recovery [17].

2.7. In vitro release profiles of ART from γ-CD-C_{10} nanocarriers

The water was kept as release medium. The saturating concentration of ART in the water at 37 °C was experimentally determined at 0.098 mg mL^{-1}. On this basis, all the drug release experiments were performed to ensure that the maximum concentration corresponding to 100% ART release did not exceed 0.065 mg mL^{-1}.

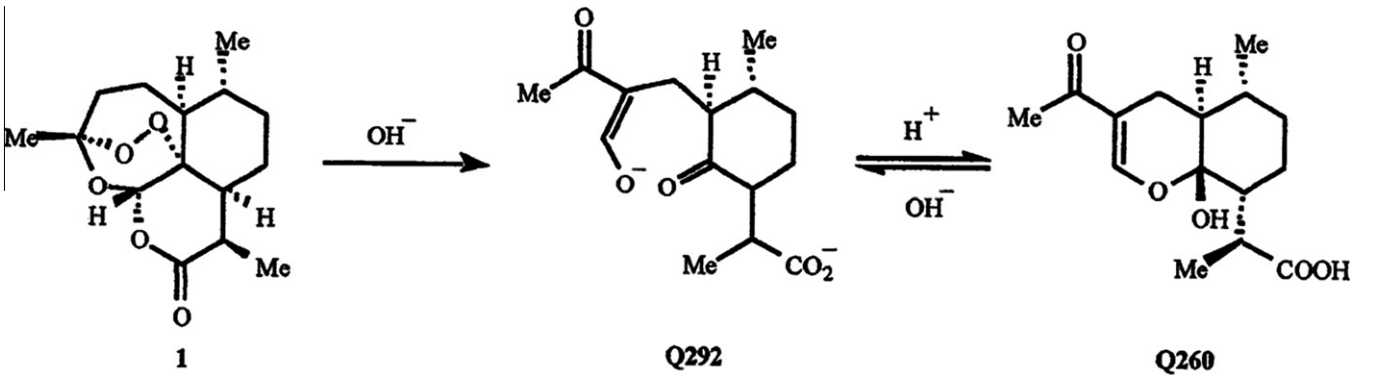

Fig. 3. ART conversion into the ultraviolet (UV) active compound Q260 [16]. ART compounds absorb in the UV region between 210 and 220 nm with poor molar extinction coefficients. Standard UV detection methodology is therefore ineffective in their quantification. The detection of ART has been performed by using pre- or post-column derivatization to convert the drug into a UV active compound that absorbs with a large extinction coefficient at longer wavelengths).

Freshly prepared ART-loaded γ-CD-C_{10} based colloidal suspensions (nanospheres and nanoreservoirs) were introduced into the release medium (100 or 125 mL of deionized water) under agitation at 50 rpm at 37 °C. At given time intervals, a sample was taken from the medium and ultracentrifuged at 300,000 g (spheres) or 400,000 g (reservoirs), at 20 °C for 1 h. The amount of ART in the supernatant was determined by HPLC coupled to evaporative light scattering detection (ELSD) [18] (Varian Prostar pump; ELSD SEDEX Model 55 Touzart & Matignon, France; 20 μL sample loop; reversed-phase Kromasil C_{18} 250 × 4.6 mm silica column, 5 mm particle size (SUPELCO INC); methanol–water (70:30, v/v) as mobile phase; 1 mL min^{-1} flow rate; detector temperature set at 32 °C; carrier gas pressure at 2.2 bar; signal gain at 12). The calibration curve (r^2 = 0.9937, $y = 1.6569x + 0.8847$) was generated by plotting the logarithm of area under the curve versus the logarithm of concentration. ART-loaded γ-CD-C_{10} based nanosystems demonstrated a good stability after centrifugation. These conditions allowed to separate particles from the supernatant and ART in the supernatant.

2.8. In vitro antimalarial activity of ART-loaded γ-CD-C_{10} based nanosystems

The *P. falciparum* susceptibility to ART-loaded nanosystems was performed using two parasite strains: a chloroquine-resistant K1 strain and a chloroquine-sensitive 3D7 strain. These two strains were cultured *in vitro* in 25 cm^2 3055 corning flasks (USA) with washed erythrocytes (blood of human O rhesus (+) group collected on heparin, obtained from national center of blood transfusion of Burkina Faso and used within 7 days when stored at 4 °C) at a 2% hematocrit in complete culture medium at 37 °C in 5% CO_2, 2% O_2, and 93% N_2 atmosphere. This medium contained RPMI 1640 supplemented with 0.25% Albumax® II, 25 mM $NaHCO_3$, 50 μg L^{-1} gentamicin, and 25 mM HEPES buffer (pH 7.4). The parasitemia was monitored daily by microscopic observation of Giemsa-stained thick blood smears and maintained between 2 and 6% by dilution with non-infected O^+ erythrocytes if necessary [19,20].

The stock solutions of the tested products (colloidal suspensions and reference antimalarial drugs) were extemporaneously prepared in appropriate solvents at various drug initial concentrations: ART-loaded particles (100 ng mL^{-1}) in complete culture medium, Artemisinin (ART, 49.6 nmol L^-), Dihydro-artemisinin (DHA, 25.6 nmol L^{-1}), and quinine hydrochloride (Q, 800 nmol L^{-1}) in methanol, chloroquine diphosphate (CQ, 1600 nmol L^{-1}) in sterilized distilled water. In the case of lipophilic reference drug stock solutions, less than 1% methanol was present in the final concentration contained, which was found to be non-toxic to the parasite [19,21]. The solutions were distributed on 96-well culture microplates (353072-BD, Falcon®) to obtain serial dilutions with complete culture medium (100 μL). Parasitized erythrocytes were used as growth control (positive control) and non-parasitized erythrocytes as negative control. Parasite growth was assessed in duplicate for each serial dilution [20,21] by addition of parasitized blood culture (2% hematocrit and 1.5% parasitemia, 100 μL) to each well. Incubation was performed at 37 °C in 5% CO_2 atmosphere during 72 h [21].

The parasite growth in each well was determined by measuring the activity of the *plasmodium*-lactate dehydrogenase (pLDH) according to the method developed by Makler et al. [22]. Briefly, at the end of incubation, the culture was homogenized and an aliquot of 20 μL was taken and transferred to another 96-well plate. 100 μL of Malstat reagent and 25 μL of NBT/PES solution were then added to the medium. The color development in the plate was monitored colorimetrically by optical densities measurement at 650 nm using spectrophotometer plate reader (ELx 808-BioTek). The drug activity, expressed as the concentration of drug that inhibited parasite growth by 50% (IC_{50}), was determined from dose–response curves obtained using Table Curve software 2D v.5.0.

2.9. Statistical analysis

All results were expressed as mean value ± standard deviation (SD). The ANOVA variance analysis was applied to repeated measurements to compare the characteristics of particles and *in vitro* release data at specific time intervals. The level of significance (P) was set at 5%.

3. Results and discussion

3.1. Formulation and characterization of nanospheres

We first investigated the influence of oligosaccharide ring size (β or γ) and initial CD-C_{10} concentration (FI = 1 mg mL^{-1} or FII = 2 mg mL^{-1}) on the physicochemical characteristics of the particles, in the conditions of nanoprecipitation. Both β- and γ-CD-C_{10} fatty esters formed monodisperse supramolecular nanoaggregates with a size of around 100 nm (Table 1), in agreement with previous observations [13]. The ability of CD-C_{10} nanoaggregates to entrap ART was thus evaluated in the absence of surfactant classically used to stabilize these nanosystems.

The CD concentration in the organic phase did not influence the mean particle size but affected the drug recovery. When ART (5 mg) was introduced in the formulation, the drug loading values expressed in terms of drug recovery (DR), drug association (DA), and entrapment efficiency (EE) were higher for γ-CD-C_{10} at the initial CD concentration of 2 mg mL^{-1} in the organic phase (FII). Indeed, the particles exhibited high drug association percentage close to 90% with a total concentration of ART recovered in the suspension of 0.43 mg mL^{-1}. It has to be noted that a slight fraction of ART remained in the aqueous phase corresponding to the experimentally determined ART hydrosolubility at 25 °C (0.064 mg mL^{-1}). A slight

Table 1
Characteristics of unloaded and ART-loaded nanospheres made from β- and γ-CD-C_{10}.

	β-CD-C_{10}				γ-CD-C_{10}			
	Unloaded particles		ART-loaded particles		Unloaded particles		ART-loaded particles	
	F I	F II	F I	F II	F I	F II	F I	F II
Mean particle size (nm, n = 3)	98 ± 9	104 ± 6	103 ± 6	105 ± 7	85 ± 8	88 ± 5	111 ± 7	106 ± 4
Mean PI (n = 3)	0.06	0.04	0.05	0.04	0.04	0.09	0.07	0.05
ζ (mV)	−27 ± 4	−30 ± 2	−20 ± 2	−21 ± 1	−26 ± 1	−26 ± 1	−19 ± 1	−18 ± 2
Ct (mg mL^{-1})	–	–	0.23	0.27	–	–	0.27	0.43
Associated ART = Qt − Qs (mg)	–	–	0.85	1.84	–	–	1.32	3.26
DR (%)	–	–	23.00	46.80	–	–	33.80	72.00
DA (%)	–	–	73.91	78.63	–	–	78.11	90.56
EE (%)	–	–	8.50	9.20	–	–	13.20	16.30

increase in particle mean size and a slight decrease in zeta potential absolute value were observed in the presence of ART suggesting that part of drug molecules was adsorbed on the particle surface.

The high drug EEs of γ-CD-C_{10} particles (13.2 (FI) and 16.3% (FII)) compared to those obtained with β-CD-C_{10} (8.5 (FI) and 9.2% (FII)) may be explained by a specific interaction between ART and the γ-CD-based systems. It is assumed that there are several sites for the drug location within the nanostructures. Indeed, the hypothesis of fixation of the drug to specific sites via hydrophobic bonds has been discussed by Lemos-Senna et al. [23]. It is also quite likely that part of the drug interacts with the cavity of CD-C_{10}, although this hypothesis remains to be confirmed.

The TEM images of negatively stained preparations revealed that the γ-CD-C_{10} nanoparticles (ART-loaded or not) were spherical (Fig. 4d and c, respectively), whereas the corresponding β-CD-C_{10} particles were mostly barrel-shaped (Fig. 4b and a, respectively). This barrel morphology has recently been shown to correspond to a specific hexagonal organization of the β-CD-C_{10} molecules, correlated with the degree of substitution of the derivative [15]. Regarding γ-CD-C_{10}, X-ray diffraction studies are in progress to determine the supramolecular organization and the interaction of ART within the nanostructure.

On the basis of EE results, the systems prepared from γ-CD-C_{10} in the FII conditions (2 mg mL^{-1}) were selected for further experiments.

It is well known that the solvent displacement technique allows to associate significant amounts of drug with a large part that is adsorbed on the surface [23]. Once the formulation realized, a drug desorption from the particles has been observed over time. In order to avoid this loss of drug, we investigated the influence of an additional coating layer of CDs on the preformed particles. The influence of the incorporation mode (one step or two steps) on ART recovery and stability of these formulations were thereby evaluated. As seen in Fig. 5, smaller particles were obtained when drug was co-nanoprecipitated with γ-CDs (processes 1 and 2) without noticeable influence of the overall CD amount introduced (20 and 30 mg, respectively).

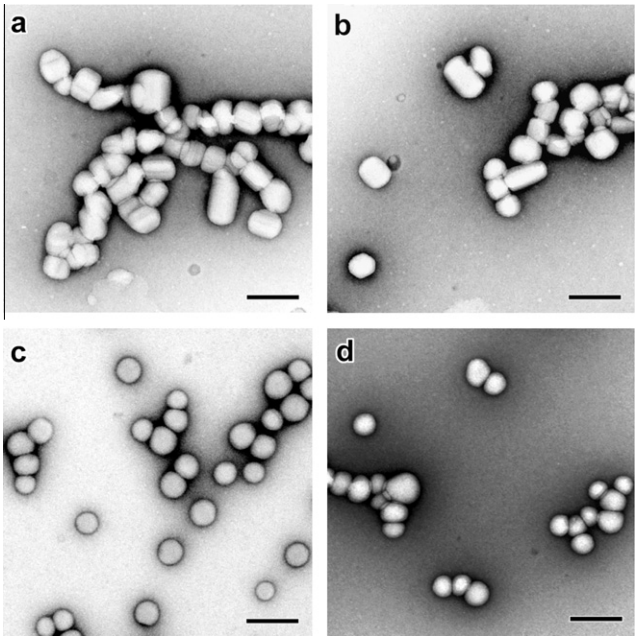

Fig. 4. TEM images of negatively stained particles: (a) β-CD-C_{10}, unloaded; (b) β-CD-C_{10}, ART-loaded; (c) γ-CD-C_{10}, unloaded; (d) γ-CD-C_{10}, ART-loaded. Scale bars: 200 nm.

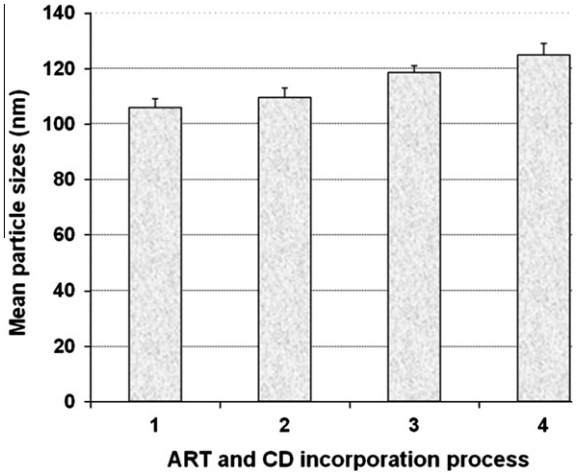

Fig. 5. γ-CD-C_{10} particle size (mean ± SD) as a function of ART and CD incorporation process.

The nanoparticles prepared by incorporating CD in two steps (20 mg then 10 mg) displayed better initial ART recovery percentages (Fig. 6). Indeed, 84 and 85% DRs were, respectively, obtained in the cases of processes 2 and 4, against 72% and 56% initial DRs for processes 1 and 3. However, whatever the process involved, a loss of drug was observed during the first 14 days, more pronounced in the case of processes 3 and 4, until a stable drug dosage was reached in each type of suspension (Fig. 6). At day 30, total ART amounts of 2.04, 2.70, 1.41, and 2.20 mg were recovered in the suspensions prepared with processes 1, 2, 3, and 4, respectively, corresponding to DRs of 46, 61, 34, and 51%.

This loss may be explained by desorption of part of the drug adsorbed at the surface of particles. When ART-loaded nanospheres were formulated in the conditions of processes 1 and 2 with a lower initial drug amount corresponding to the drug amount remaining at day 14, a high DR (95%) was measured corresponding to ART doses of 0.24 and 0.31 mg mL^{-1}, respectively. These latter formulations were stable over at least 1 month.

It has to be noted that the amount of recovered ART was higher when process 2 (two-step addition of 20 + 10 mg of CD) was used. To understand this phenomenon, a new formulation was performed by a one-step addition of 30 mg of CD. The corresponding particle characteristics (mean size = 106 nm, PI = 0.10, Ct = 0.31 mg mL^{-1}) were similar to those obtained with process 2. The high concentration of ART in the suspension obtained with process 2 was related

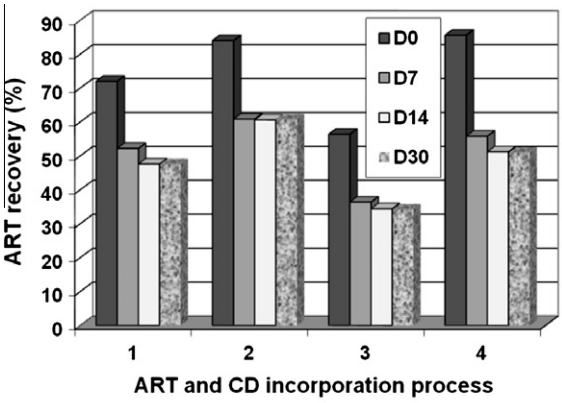

Fig. 6. Drug recovery of loaded γ-CD-C_{10} nanoparticles over 30 days for each process.

to the CD amount introduced. This observation showed that the multi-step introduction of CD did not impact the physicochemical characteristics and stability of particles. Moreover, the results suggest the existence of a drug amount compatible with the formulation of stable nanoparticles. This particular drug amount seems related to the CD material proportion involved in the formulation corresponding to a molar ratio CD/ART of 1:1. Above this equilibrium conditions, an excess drug amount may still be associated with the nanosystem via stacking layers, but non-permanently, thus leading to desorption.

3.2. Formulation and characterization of reservoir-type nanosystems

The high solubility and the good chemical stability (performed at 25 °C and 4 °C for 60 days) at room temperature of ART in benzyl benzoate (BB) (83.30 mg mL^{-1}) compared to medium chain triglycerides (Miglyol 812 N, 23.10 mg mL^{-1}) prompted us to use BB (200 μL) as internal phase of the nanoreservoirs. First, conventional conditions were used to prepare nanoreservoir suspensions involving a low initial CD concentration (2 mg mL^{-1}) and a high lipophilic/hydrophilic surfactant amounts (80 mg/80 mg) [13]. Stable nanoreservoir systems with 190 nm mean particle size were prepared. The amphiphilic molecules (γ-CD-C_{10} and surfactant) were assumed to form a membrane layer surrounding the lipophilic internal phase. This formulation showed a good ability to associate ART with drug recovery percentage around 92%. The following objective was to optimize the formulation by decreasing the surfactant amount in order to ensure injectable polysorbate concentration within the final suspension [24]. The preparation of optimized suspensions of monodisperse nanoreservoir particles with a size lower than 200 nm presenting a high drug recovery was highly dependent of the proportion of amphiphilic compounds. The screening experiments showed that it was possible to obtain stabilized formulations while lowering the surfactant amount and increasing CD initial concentration (4 mg mL^{-1}). In this condition, the threshold amount of surfactant required for a stable formulation was evaluated at 20 mg. As seen in Table 2, the presence of ART in these formulations did not modify the average particle diameter, suggesting that the drug was mainly localized in the lipophilic core. The zeta potential absolute value did not significantly vary. The amount of entrapped drug was higher than that obtained with nanospheres. The highest drug concentration in the colloidal suspension (1.68 mg mL^{-1}, DR = 94.02%) was obtained in the conditions of formulation C (40 mg γ-CD-C_{10}, 40 mg Montanox® 80 and 40 mg Montane® 80). Furthermore, the average diameter of reservoir-type particles increased with the amount of BB. Unstable formulations were obtained from 400 μL of BB (data not shown).

Like other nanosystems reported in the literature such as polymeric nanocarriers [25], amphiphilic β-CD nanoparticles [26], lipid nanocapsules [27], the γ-CD-C_{10} ART-loaded nanoreservoirs stored at room temperature present a good physicochemical stability during at least 1 month.

The TEM images of negatively stained ART-loaded nanoreservoirs (formulation C) suggest that the particles flattened and coalesced during drying (Fig. 7a), as previously reported [13]. Consequently, the size cannot be reliably measured. A population of significantly smaller particles (about 5 nm in diameter) was also observed, likely corresponding to surfactant micelles. To prevent drying artifacts, cryo-TEM images of the quench-frozen suspension were recorded (Fig. 7b). Individual spherical particles were observed, with a diameter typically ranging from 40 to 300 nm. The micelles observed for the negatively stained sample were probably too small to be detected in the cryo-TEM image. If we assume that the ice film has a thickness of 100–150 nm, it is likely that the soft particles with an apparent diameter larger than this value flattened in a direction perpendicular to the film plane, which would shift the size distribution toward higher values. Nevertheless, the apparent size distribution is in agreement with the values determined by dynamic light scattering (DLS).

3.3. Formulation and characterization of PEGylated nanocarriers

Gèze et al. previously demonstrated that nanoparticles made from amphiphilic CDs were rapidly cleared from bloodstream following their systemic administration in mice, resulting from their interactions with mononuclear phagocyte system (MPS), and accumulated in the liver and spleen [28]. It has clearly been demonstrated that nanoparticles with a hydrophilic surface induced a significant decrease in the opsonization process and recognition by MPS and plasma proteins [29–31]. To prepare γ-CD-C_{10} nanodevices decorated on the surface, we used PEG fatty acid ester. Indeed, PEG is a well-known hydrophilic polymer playing a key role in the prevention against the removal by MPS via a repulsive steric effect [32–34]. The idea of using PEG grafted with alkyl chain (PEG fatty acid ester) is to create an efficient anchoring of amphiphilic PEG in the carrier, via strong hydrophobic interaction between the alkyl chain of PEG ester and the aliphatic part of amphiphilic CD forming the nanosystems.

γ-CD-C_{10} derivative formulated with low molecular weight PEG (300 or 400 Da) esters (dilaurate, stearate) was unstable in the presence of electrolytes (NaCl 0.09%), as already observed in the case of non-PEGylated nanospheres (results not shown). To the contrary, stable suspensions of nanospheres were obtained with high chain length PEG stearate (1500 and 4000 Da) in presence of NaCl. In the latter case, the size of particles increased with the amount of PEG ester introduced in the formulation. These observations are in good agreement with previous reports claiming that the PEG chain length must exceed 1000 Da for an effective stabilization of nanocarriers [33]. Then, PEGylated nanoreservoir systems were formulated by varying the amount of the following constituents of formulation: γ-CD-C_{10}, Montane® 80, Montanox® 80 and PEG4000 stearate. The best drug recovery percentage was obtained in the cases of formulations PNR1 (40 mg γ-CD-C_{10}, 40 mg Montane® 80 and 15 mg PEG4000 stearate) and formulation PNR2 (20 mg γ-CD-C_{10}, 40 mg Montane® 80, 40 mg Montanox® 80

Table 2
Unloaded and ART-loaded γ-CD-C_{10} nanoreservoir characteristics.

	Formulation content (mg)			Unloaded nanoreservoirs			ART-loaded nanoreservoirs				
	γ-CD C_{10}	Montanox 80	Montane 80	Mean size (nm)	PI	ζ (mV)	Mean size (nm)	PI	ζ (mV)	Ct (mg/mL)	DR (%)
A	20	80	80	190 ± 8	0.08	−24 ± 1	185 ± 6	0.04	−23 ± 1	1.51	91.88
B	20	40	40	180 ± 4	0.04	−27 ± 1	181 ± 7	0.06	−26 ± 1	1.19	84.24
C	40	40	40	176 ± 4	0.05	−30 ± 1	177 ± 6	0.04	−28 ± 1	1.68	94.02
D	40	30	30	177 ± 9	0.07	−29 ± 1	177 ± 8	0.06	−28 ± 1	1.54	92.67
E	40	20	20	179 ± 6	0.05	−30 ± 1	179 ± 4	0.03	−27 ± 1	1.29	85.13
F	40	20	10	177 ± 9	0.06	–	Unstable formulation was obtained				

Volume of BB = 200 μL.

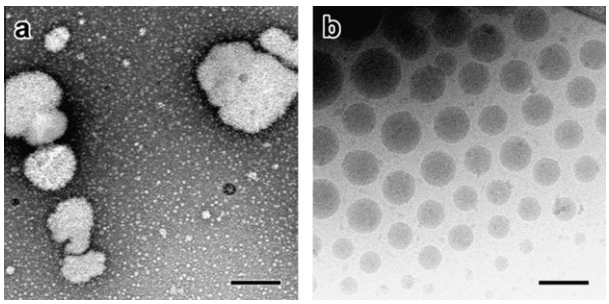

Fig. 7. TEM images of ART-loaded γ-CD-C_{10} nanoreservoir systems: (a) negative staining; (b) cryo-TEM. Scale bars: 200 nm.

and 15 mg PEG4000 stearate). The particle characteristics for each formulation are summarized in Table 3. The CD/PEG ester ratio used was 4:1 and 8:3 (w/w) for nanosphere and nanoreservoir suspensions, respectively.

In agreement with previous studies [34], the introduction of PEG4000 stearate induced a weak increase in the average diameter of particles and a decrease in the potential zeta absolute value of sphere nanosystems from −26 to −13 and from −18 to −10 for unloaded and ART-loaded nanospheres, respectively, prepared by using process 1 (Tables 1 and 3). These results suggest the presence of PEG moieties at the surface of the particles, creating a steric barrier against flocculation in an electrolyte rich medium. The PEGylation was also applied to the derivative β-CD-C_{10}, in presence of PEG4000 stearate, leading to the same observations.

In comparison with the optimized ART-loaded nanosphere formulated without any stabilizing agent, the amount of ART recovered with γ-CD-C10 PEGylated particles increased from 0.24 to 0.34 mg mL^{-1} and from 0.31 to 0.47 mg mL^{-1} in the conditions of processes 1 and 2, respectively. As demonstrated in a previous study [13], the presence of stabilizer such as polyoxyethylated derivatives improved the association by promoting contact between the drug and the hydrophobic particle surface. As can be seen in the TEM images of negatively stained preparations, PEGylated particles (ART-loaded or not) are faceted, although the average size did not significantly change (Fig. 8).

The effect was not clearly detected on the particles prepared from β-CD-C_{10} derivative (Fig. 8a and b, respectively) as their barrel shape was preserved. The faceting of γ-CD-C_{10} particles may be due to the organization of PEG chains that, depending on their density on the surface of the particles, would form a more or less contiguous rigid layer (Fig. 8c and d).

The introduction of PEG esters species in the formulation did not modify the ability to entrap ART. Indeed, the DR value was higher than 90%. It has to be noted that PEG4000 stearate nanoparticles showed good stability in terms of size distribution and amount of associated drug after a 30-day storage at room temperature (data not shown). The TEM images of negatively stained PEGylated nanoreservoirs show a polydisperse distribution of particles. However, the flattening and coalescence are less marked than in the case of non-PEGylated γ-CD-C_{10} reservoirs suggesting that PEG rigidified the surface of the soft particle (Fig. 9a). The cryo-TEM images of the ice-embedded PEGylated ART-loaded nanoreservoirs confirmed the polydispersity of the particles (Fig. 9b), with a size ranging from 40 to 400 nm. Again, the larger particles likely flattened in the ice film which shifts the size distribution toward higher values.

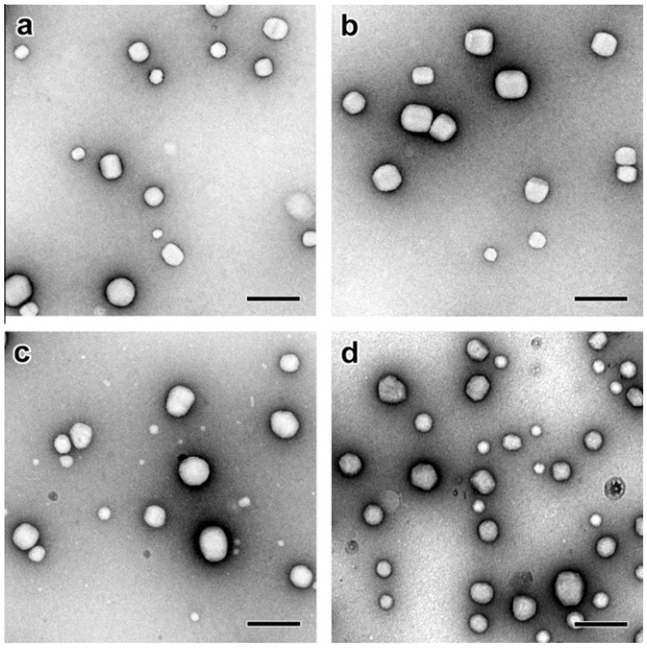

Fig. 8. TEM images of negatively stained PEGylated (PEG 4000 stearate) nanospheres: (a) β-CD-C_{10}, unloaded; (b) β-CD-C_{10}, ART-loaded; (c) γ-CD-C_{10}, unloaded; (d) γ-CD-C_{10}, ART-loaded. Scale bars: 200 nm.

Schematic representations of the γ-CD-C_{10} nanosystems were drawn based on these results (Fig. 10). In the case of nanospheres, the γ-CD-C_{10} molecules form a dense structure whose supramolecular organization has not been elucidated yet. The host drug molecule can be located in different regions of the nanostructure, namely adsorbed on the surface and/or entrapped within the core. Drug interaction with the CD cavity may also be possible, via interaction with the primary face of the γ-CD that is less hindered than the secondary face. Indeed, γ-CD complexes at a CD:ART molar ratio of 1:1 were described by Wong and Yuen [5]. In the case of PEGylated nanospheres, the stearate chains of the PEG fatty acid ester are thought to strongly interact with the internal structure

Table 3
Characteristics of PEGylated (PEG4000 stearate) nanosystems.

Formulations	Mean size (nm)	PI	ζ (mV)	Ct (mg/mL)	DR (%)	DA (%)
Unloaded nanosystems stabilized by PEG4000 stearate						
PNS (process 1)	105 ± 4	0.07	−13 ± 1	–	–	–
PNS (process 2)	107 ± 5	0.07	−13 ± 2			
PNR1	203 ± 8	0.04	−16 ± 2	–	–	–
PNR2	190 ± 4	0.03	−19 ± 1	–	–	–
ART-loaded nanosystems stabilized by PEG4000 stearate						
PNS (process 1)	113 ± 6	0.05	−10 ± 1	0.34	79.33	87.40
PNS (process 2)	115 ± 8	0.07	−9 ± 2	0.47	80.41	88.00
PNR1	205 ± 7	0.09	−23 ± 3	1.52	92.04	96.33
PNR2	191 ± 9	0.08	−23 ± 2	1.49	91.88	95.25

PNS = PEGylated nanospheres, PNR = PEGylated nanoreservoirs.

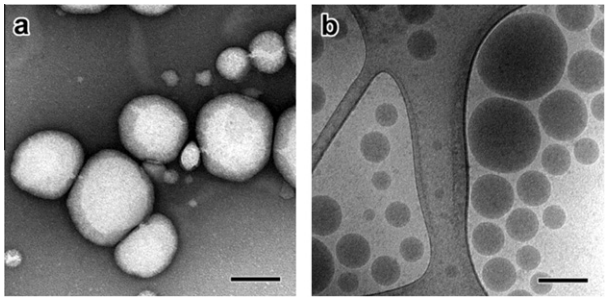

Fig. 9. TEM images of PEGylated (PEG4000 stearate) ART-loaded γ-CD-C_{10} nanoreservoirs: (a) negative staining; (b) cryo-TEM. Scale bars: 200 nm.

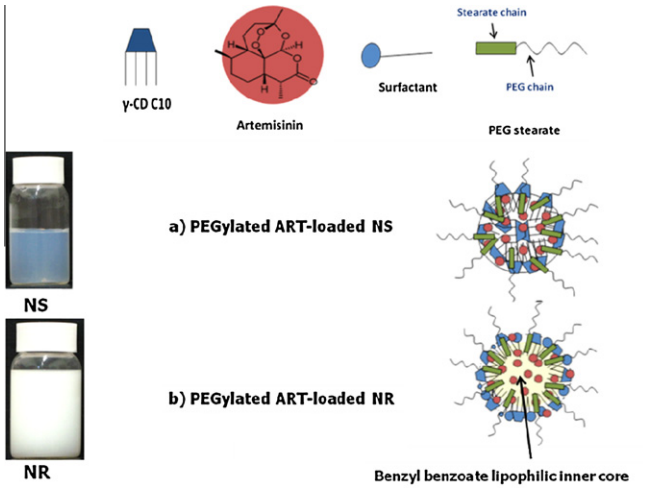

Fig. 10. Photographic images of colloidal suspensions (NS = nanosphere, NR = nanoreservoir) and schematic representation of PEGylated ART-loaded nanosphere (a) and PEGylated ART-loaded nanoreservoir (b). (For interpretation of the references to color in this figure legend, the reader is referred to the web version of this article.)

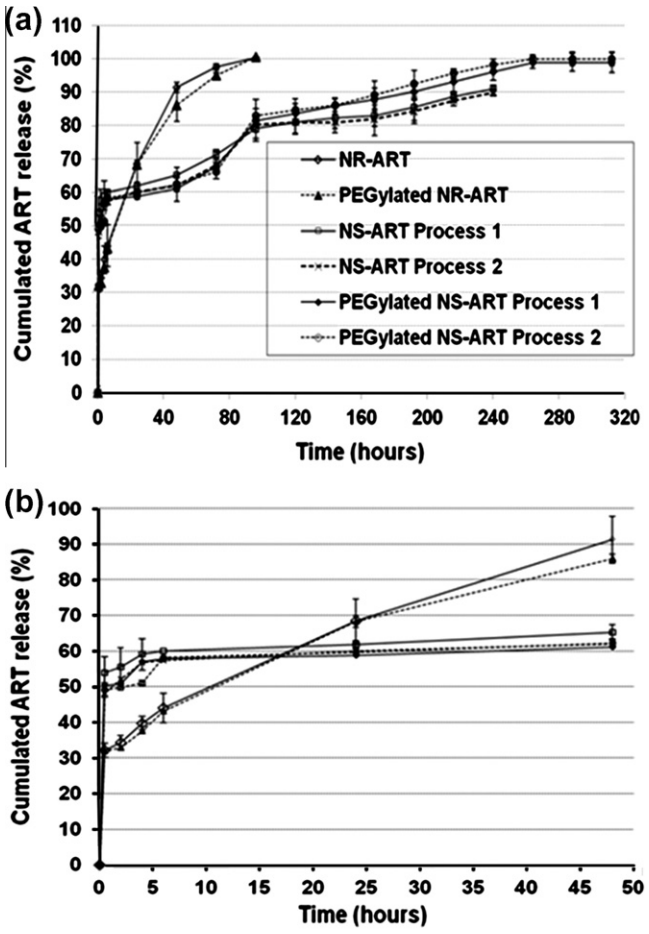

Fig. 11. *In vitro* release profiles of ART from γ-CD-C_{10}-based sphere and reservoir-type nanosystems (n = 3, SD) (a) and *in vitro* release profiles during the first 48 h (b). PEGylated NR-ART = PNR1.

of amphiphilic CD, whereas polyoxyethylene portions protrude out in the aqueous phase (Fig. 10a).

The nanoreservoir systems are constituted by a lipophilic core corresponding to the BB solution of ART that is surrounded by the shell of amphiphilic molecules (γ-CD-C_{10}, Montane® 80, Montanox® 80, PEG stearate). The aliphatic part of the amphiphilic molecules is considered to be anchored in the BB phase, while the hydrophilic part is located in the aqueous solution (Fig. 10b). Moreover, a part of the drug can be attached to the shell of the nanoreservoirs or adsorbed on their surface.

3.4. In vitro release

In *vitro* release assessment was performed on six ART-loaded γ-CD-C_{10} nanoparticulate formulations: γ-CD-C_{10} nanospheres made by processes 1 and 2 without any surfactant (NS-ART), PEG4000 stearate/γ-CD-C_{10} nanospheres made by processes 1 and 2 (PEGylated NS-ART), Montane® 80/Montanox® 80/γ-CD-C_{10} nanoreservoirs (NR-ART) and Montane® 80/PEG4000 stearate/γ-CD-C_{10} nanoreservoirs (PEGylated NR-ART). ART release from nanocarriers has been assessed using the dilution–centrifugation method [35]. As seen in Fig. 11, γ-CD-C_{10} sphere and reservoir-type nanosystems exhibited a sustained ART release profiles. For both systems, a burst effect was observed (50% or 32% of drug release, respectively).

The γ-CD-C_{10} based nanospheres showed a significant sustained release profile of ART extended up to 11 days. The rapid initial release of ART from particles (50% after 30 min) could be attributed to free solubilized ART and drug located near the surface of nanocarriers. The delayed release may be related to drug located within the matrix structure of nanospheres. The sustained release of drug from particles indicated that ART was more sequestered by the nanostructure. There might be a strong interaction between ART and γ-CD-C_{10} nanocarriers. As previously suggested, the interaction with the cavity of γ-CD-C_{10} may be considered. The influence of the size of cavity of modified CD has been observed in a previous release study involving diazepam (DZ) loaded CD-C_{10} nanospheres. The *in vitro* DZ sustained release was more pronounced in the case of γ-CD-C_{10} in comparison with DZ loaded α- and β-CD-C_{10} nanospheres [13]. So the drug was more retained by the γ-CD-C_{10} nanostructure. Besides the CD ring size and the drug itself, the site of CD modification seems to influence the drug release from amphiphilic β-CD nanocarriers. Indeed, different release profiles of camptothecin from β-CD-C_6 (modified on the secondary face) and 6-O-Capro-β-CD (modified on the primary face) nanoparticles were obtained by Cirpanli et al. [36]. Both camptothecin-loaded nanoparticles exhibited a biphasic release comprising an initial burst (30% after 2 and 5 h, respectively) followed by a sustained phase extended up to 6 or 12 days, respectively. In turn, all these parameters may influence the internal self-organization of CD molecules, the accessibility of the oligosaccharides by the drug, its location within the nanostructure and thus its drug release from the nanocarrier. We have recently revealed a correlation between

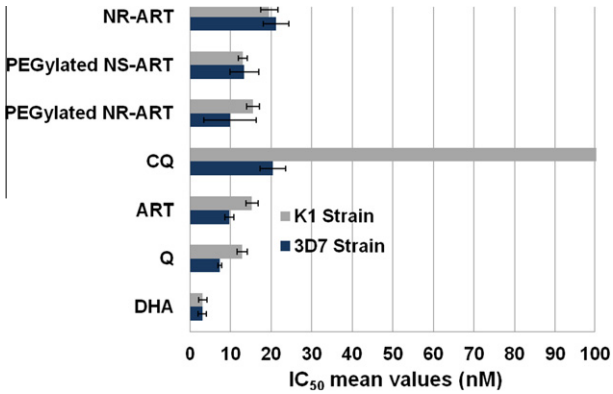

Fig. 12. IC_{50} values (nM) of ART-loaded nanosystems and references drugs on 3D7 and K1 strains of *P. falciparum*. The measured IC_{50} of CQ on the strain K1 = 227.8 nM. The IC_{50} cutoff values used to define resistance of reference drug: DHA > 30 nM, ART > 30 μg/mL (>106 nM), CQ > 100 nM, Q > 500 nM. (For interpretation of the references to color in this figure legend, the reader is referred to the web version of this article.)

the substitution degree of β-CD-C_{10} and the internal structure of formulated nanospheres [15]. Lamellar and hexagonal supramolecular organizations were identified by small-angle X-ray scattering and TEM for β-CD-C_{10} characterized by DSs of 3.8 and 6.6, respectively. In this context, the study of the ultrastructure of the unloaded and loaded γ-CD-C_{10} nanosphere suspension is a key point to better understand the way the host and guest interact. This will be the object of another study.

In the present study, the slight differences observed in the median values between the two processes (1 and 2) release data were not statistically significant ($P \geqslant 0.200$). In addition, the stabilization of nanoparticles with PEG4000 stearate did not significantly influence the release profiles of ART from nanocarriers during the first period. The incomplete cumulated ART release (90%) exhibited by non-PEGylated nanospheres was the consequence of nanosphere flocculation occurring at day 10.

ART associated with the nanoreservoirs was released during a period of approximately 96 h. About 30% of drug was released into the aqueous medium after 30 min. These release kinetics displayed then a slower profile over 96 h. The slow release profile of the remaining drug suggested that the release of drug located within lipophilic core of the reservoirs is mainly governed by the drug partition between the oil core and the aqueous external medium and the diffusion of drug through the reservoir shell.

The results of the ART release from the nanocarriers were very reproducible. The biphasic release profiles are expected to meet a rapid high dose of ART (in cases of severe malaria) together with ART plasma levels over a prolonged period owing to the hydrophilic PEG corona.

3.5. In vitro antimalarial activity

The ART-loaded nanoparticles and the reference drugs were assayed against 3D7 and K1 strains of *P. falciparum*. Non-PEGylated ART-loaded nanospheres were not assayed for antimalarial activity since they were unstable in RMPI medium.

The IC_{50} values obtained after correlation with *in vitro* release results are reported in Fig. 12. The order of activity of the reference drugs against both strains was as follows: DHA < Q < ART < CQ. The two strains of *P. falciparum* were highly sensitive to ART-loaded nanosystems with low IC_{50} values. The mean IC_{50} values were in the range 9.9–21.3 nM (2.8 and 6.0 ng mL^{-1}). The strain 3D7, which is susceptible to chloroquine, yielded IC_{50} values of 9.9, 13.4, and 21.3 nM, respectively, for PEGylated nanoreservoirs, PEGylated NS made by process 1, and non-PEGylated nanoreservoir systems, whereas the strain K1, which is resistant to chloroquine, showed IC_{50} values of 15.6, 13.0, and 19.5 nM, respectively. The *in vitro* activities against 3D7 and K1 strains of all ART-loaded colloidal suspensions were significantly comparable to that of ART reference (IC_{50} = 9.8 nM (3D7) and 15.3 nM (K1), $0.001 \leqslant P \leqslant 0.02$), excepted for non-PEGylated ART-loaded nanoreservoir suspension. However, the high IC_{50} values in the latest case (21.3 nM and 19.5 nM on the strains 3D7 and K1 respectively) was in the range of ART sensitivity (sensitivity threshold of the ART = 106 nM). In another hand, all the tested ART-loaded colloidal suspensions were more active than chloroquine drug even on the chloroquino-sensitive strain.

The results from this study indicate that ART-loaded nanosystems, mainly PEGylated ones exhibit satisfactory *in vitro* activity against Chloroquine-sensitive and chloroquine-resistant strains of *P. falciparum*. These findings suggest that neither additive nor antagonistic effect was observed when ART was associated with γ-CD-C_{10} nanocarriers. In addition, the OD values obtained with unloaded nanocarriers were comparable to those of negative control, suggested that γ-CD-C_{10} nanocarriers have no effect on parasite growth in the test conditions. However, this assumption must be confirmed by a cytotoxic study, which will determine the selectivity index (ratio between cytotoxic and antimalarial activities).

4. Conclusion

Biosynthesized β- and γ-CD-C_{10} are able to form supramolecular assemblies such as nanospheres and reservoir-type nanosystems in the conditions of solvent displacement. PEG surface-decorated nanostructures were developed via the interaction of PEG fatty acid esters of different chain length and CD-C_{10} derivatives. The two types of developed nanostructures were able to associate artemisinin. Stable formulations associated with high drug content were obtained with γ-CD-C_{10}. *In vitro* release characteristics showed an extended release from 4 to 12 days, which was not influenced by the presence of the hydrophilic corona. *In vitro* antimalarial activity data indicate that both ART-loaded nanosystems are potentially interesting for clinical applications. These colloidal nanocarriers may provide a promising alternative for injectable use of ART. *In vitro* cytotoxicity, complement activation, and macrophage uptake as well as biodistribution studies are in progress in order to assess the safety and stealthiness of these colloidal drug delivery systems.

Acknowledgments

The authors thank Christine Brunet-Manquat and Delphine Levilly (DPM) as well as Paul Lamoussa Ouattara (CNRFP) for their technical assistance. We also thank the French Embassy in Burkina Faso for the financial support of Josias Yaméogo.

References

[1] World Health Organization (WHO), Management of Severe Malaria: A Practical Handbook, second ed., 2000, 84p.
[2] M.E. Van Agtmael, T.A. Eggelte, C.J. van Boxtel, Artemisinin drugs in the treatment of malaria: from medicinal herb to registered medication, TiPS 20 (1999) 199–205.
[3] J.F.S. Ferreira, J. C Laughlin, N. Delabays, P.M. Magalhaes, Cultivation and genetics of *Artemisia annua* for increased production of the anti-malarial artemisinin, Plant Genet. Resour. 3 (2005) 206–229.
[4] J.W. Wong, K.H. Yuen, Inclusion complexation of artemisinin with α-, β- and γ-cyclodextrins, Drug Dev. Ind. Pharm. 29 (2003) 1035–1044.
[5] J.W. Wong, K.H. Yuen, Improved oral bioavailability of artemisinin through inclusion complexation β- and γ-cyclodextrins, Int. J. Pharm. 227 (2001) 177–185.

[6] N.G. Sahoo, A. Abbas, Z. Judeh, C.M. Li, K.-H. Yuen, Solubility enhancement of poorly water-soluble antimalarial drug: experimental design and use of a modified multifluid nozzle pilot spray drier, J. Pharm. Sci. 98 (1) (2009) 281–296.
[7] B. Chimanuka, M. Gabriels, M.-R. Dtaevernier, J.A. Plaizier-Vercammen, Preparation of β-artemether liposomes, their HPLC-UV evaluation and relevance for clearing recrudescent parasitemia in *Plasmodium chabaudi* malaria-infected mice, J. Pharmaceut. Biomed. Anal. 28 (2002) 13–22.
[8] M. Gabriels, Physical and chemical evaluation of liposomes, containing artesunate, J. Pharm. Biomed. Anal. 31 (2003) 655–667.
[9] M. Owais, G.C. Varshney, A. Choudhury, S. Chandra, C.M. Gupta, Chloroquine encapsulated in malaria-infected erythrocytes-specific antibody-bearing liposomes effectively controls chloroquine-resistant *Plasmodium berghei* infections in mice, Antimicrob. Agents Chemother. 39 (1995) 180–184.
[10] V.C.F. Mosqueira, P.M. Loiseau, C. Bories, P. Legrand, J.-P. Devissaguet, G. Barrat, Efficacy and pharmacokinetics of intravenous nanocapsules formulations of halofantrine in *Plasmodium berghei*-infected mice, Antimicrob. Agents Chemother. 48 (2004) 1222–1228.
[11] L. Choisnard, A. Gèze, B.G.J. Yaméogo, J.-L. Putaux, D. Wouessidjewe, Miscellaneous nanoaggregates made of CD esters synthesised by an enzymatic pathway, Int. J. Pharm. 344 (2007) 26–32.
[12] L. Choisnard, A. Gèze, J.-L. Putaux, Y.S. Wong, D. Wouessidjewe, Novel nanoparticles of β-cyclodextrin esters obtained by self-assembling of bio-transesterified β-cyclodextrins, Biomacromolecules 7 (2006) 515–520.
[13] A. Gèze, L. Choisnard, J.-L. Putaux, D. Wouessidjewe, Colloidal systems made of biotransesterified cyclodextrins grafted with C10 alkyl chains, Mater. Sci. Eng. C 29 (2009) 458–462.
[14] O. Arnaud, A. Boumendjel, A. Gèze, M. Honorat, E.L. Matera, J. Guitton, W.D. Stein, S.E. Bates, P. Falson, C. Dumontet, A. Di Pietro, L. Payen, The acridone derivative MBLI-87 sensitizes breast cancer resistance protein-expressing xenografts to irinotecan, Eur. J. Cancer 47 (2011) 640–648.
[15] L. Choisnard, A. Gèze, C. Vanharverbeke, J.B.G. Yaméogo, J.-L. Putaux, B. Brasme, L. Julien, S. Boulanger, C. Elfakir, D. Wouessidjewe, Physicochemical characterization of α-, β- and γ-cyclodextrins bioesterified with decanoate chains used as building blocks of colloidal nanoparticles, Biomacromolecules 12 (8) (2011) 3031–3038.
[16] S.S. Zhao, High-performance liquid chromatographic determination of artemisinin (qinghaosu) in human plasma and saliva, Analyst 112 (1987) 661–664.
[17] A. Gèze, J.-L. Putaux, L. Choisnard, P. Jehan, D. Wouessidjewe, Long-term shelf stability of amphiphilic beta-cyclodextrin nanosphere suspensions monitored by dynamic light scattering and cryo-transmission electron microscopy, J. Microencapsul. 21 (6) (2004) 607–613.
[18] B.A. Avery, K.K. Venkatesh, M. A Avery, Rapid determination of artemisinin and related analogues using high-performance liquid chromatography and an evaporative light scattering detector, J. Chromatogr. B 730 (1999) 71–80.
[19] A. Gansané, S. Sanon, L.P. Ouattara, A. Traoré, S. Hutter, E. Olivier, N. Azas, S. Traoré, I.P. Guissou, S.B. Sirima, I. Nebié, Antiplasmodial activity and toxicity of crude extracts from alternatives parts of plants widely used for the treatment of malaria in Burkina Faso: contribution for their preservation, Parasitol. Res. 106 (2010) 335–340.
[20] P. Druilhe, A. Moreno, C. Blanc, P.H. Brasseur, P. Jacquier, A colorimetric in vitro drug sensitivity assay for *Plasmodium falciparum* based on a highly sensitive double-site lactate dehydrogenase antigen-capture enzyme-linked immunosorbent assay, Am. J. Trop. Med. Hyg. 64 (5,6) (2001) 233–241.
[21] E. Fattoruso, S. Parapini, C. Campagnuolo, N. Basilico, O. Taglialatela-Scafati, D. Taramelli, Activity against *Plasmodium falciparum* of cycloperoxyde compounds obtained from the sponge *Plakortis simplex*, J. Antimicrob. Chemother. 50 (2002) 883–888.
[22] M.T. Makler, J.M. Ries, J.A. Williams, J.E. Brancroft, R.C. Piper, B.L. Gibbins, D.J. Hinrichs, Parasite lactate dehydrogenase as an assay for *Plamosdium falciparum* drug sensitivity, Am. J. Trop. Med. Hyg. 48 (1993) 739–741.
[23] E. Lemos-Senna, D. Wouessidjewe, S. Lessieur, F. Puissieux, G. Couarraze, D. Duchêne, Evaluation of hydrophobic drug loading characteristics in nanoprecipited amphiphilic cyclodextrin nanospheres, Pharm. Dev. Technol. 3 (1) (1998) 85–94.
[24] R.C. Rowe, P.J. Sheskey, M.E. Quinn, Handbook of Pharmaceutical Excipients, 6th ed., PhP, 917p.
[25] B. Heurtault, P. Saulnier, B. Pech, J.-E. Proust, J.-P. Benoit, A novel phase inversion-based process for the preparation of lipid nanocarriers, Pharm. Res. 19 (6) (2002) 875–880.
[26] F. Quaglia, L. Ostacolo, A. Mazzaglia, V. Villari, D. Zaccaria, M.T. Sciortino, The intracellular effects of non-ionic amphiphilic cyclodextrin nanoparticles in the delivery of anticancer drugs, Biomaterials 30 (2009) 374–382.
[27] M. Teixeira, M.J. Alonso, M.M. Pinto, C.M. Barbosa, Development and characterization of PLGA nanospheres and nanocapsules containing xanthone and 3-methoxyxanthone, Eur. J. Pharm. Biopharm. 59 (2005) 491–500.
[28] A. Gèze, L. Tieu Chau, L. Choisnard, J.P. Mathieu, D. Marti-Battle, L. Riou, J.-L. Putaux, D. Wouessidjewe, Biodistribution of intravenously administrated amphiphilic β-cyclodextrin nanospheres, Int. J. Pharm. 344 (1–2) (2007) 135–142.
[29] A. Vonarbourg, C. Passirani, P. Saulnier, J.-P. Benoit, Parameters influencing the stealthiness of colloidal drug delivery systems, Biomaterials 27 (24) (2006) 4356–4373.
[30] M. E Martinez-Barbosa, S. Cammas-Marion, L. Bouteiller, C. Vauthier, G. Ponchel, PEGylated degradable composite nanoparticles based on mixtures of PEG-b-poly(γ-benzyl L-glutamate) and poly(γ-benzyl L-glutamate), Bioconjugate Chem. 20 (2009) 1490–1496.
[31] N.T. Huynh, E. Roger, N. Lautram, J.-P. Benoît, C. Passirani, The rise and rise of stealth nanocarriers for cancer therapy: passive versus active targeting, Nanomedicine 5 (9) (2010) 1415–1433.
[32] R. Grief, M. Luck, P. Quellec, M. Marchand, E. Dellacherie, S. Harnisch, T. Blank, R.H. Muller, Stealth corona-core nanoparticles surface modified by polyethylene glycol (PEG): the influence of corona (PEG chain length and surface density) and the core composition on phagocytic uptake and plasma protein adsorption, Colloids Surf. B 18 (2000) 301–313.
[33] S.M. Moghimi, A.C. Hunter, Capture of stealth nanoparticles by body's defences, Crit. Rev. Ther. Drug Carrier Syst. 18 (2001) 527–550.
[34] G.P. Zara, R. Cavalli, A. Bargoni, A. Fundaro, D. Vighetto, M.R. Gasco, Intravenous administration to rabbits of non-stealth and stealth doxorubicin-loaded solid lipid nanoparticles at increasing concentrations of stealth agent: pharmacokinetics and distribution of doxorubicin in brain and other tissues, J. Drug Target. 10 (4) (2002) 327–335.
[35] L. Polato, L.M. Benedetti, L. Callegaro, P. Couvreur, *In vitro* evaluation of nanoparticle formulations containing gangliosides, J. Drug Target. 2 (1994) 53–59.
[36] Y. Cirpanli, E. Bilensoy, A.L. Dogan, S. Calis, Comparative evaluation of polymeric and amphiphilic cyclodextrin nanoparticles for effective camptothecin delivery, Eur. J. Pharm. Biopharm. 73 (2009) 82–89.